Hydraulic Fracturing in Fill-type Dams during Earthquake

フィルダムの地震時における水理破壊現象に関する研究

Yoshio OHNE[*], Kunitomo NARITA[*]
Yoshio NAKAMURA[**] 'and Yuji MURASE[***]

大根義男, 成田国朝, 中村吉男, 村瀬裕司

ABSTRACT: In addition to the safety against sliding failure of embankment slopes, safety against internal erosion caused by hydraulic fracturing has been another important issues to be discussed in the seismic resistant design of fill-type dams. This paper concerns the mechanism and its possibility of occurrence of hydraulic fracturing in earth and rock fill dams during earthquake. Laboratory seepage fracture tests were conducted on erosive soils under various conditions of water pressure and confining stresses to know what are to be influential factors on seepage failure, and FEM dynamic response analysis was made for different cases of embankment configuration to study the extent of damages and development process of hydraulic fracturing during earthquake.

Key words: *hydraulic fracturing/ earthquake/ hydraulic gradient/ dynamic analysis/ stress ratio*

1. INTRODUCTION

Stability evaluation of fill-type dams during earthquake has mostly focused on the sliding failure of embankment slopes. FEM · dynamic response analysis has been an effective and useful tool commonly applied in the study of seismic behavior of dam body during earthquake.

In the First US-Japan Workshop on Advanced Research on Earthquake Engineering for Dams (Nov. 1996), the authors have proposed a practically useful method of stability evaluation of embankment, by taking into account response shear strain as a failure criterion.[1] Because the proposed method necessarily does not require the dynamic shear strength of construction materials, it seems to be applicable with high accuracy in the evaluation of slope stability of earth and rock fill dams.

In the earthquake resistant design of fill-type dams, however, not only stability against sliding failure of embankment slope but also that against internal erosion and water leakage through the core is necessary to ensure when the reservoir water is filled during dam operation. Cut-off wall trench construction and severe selection of core and filter zone materials are for instance to be effective measures to prevent such hydraulic fracturing damages.

In this study, laboratory seepage fracture tests were conducted to investigate failure criterion of hydraulic fracturing by paying attention on the relationship between the confining stress and hydraulic gradient in the core zone. FEM dynamic response analysis was then made on the longitudinal section of embankment dams to find stress distribution and hydraulic gradient in the core. The computed values were compared with those by tests to examine the possibility of the occurrence of hydraulic fracturing. The results presented the fact that hydraulic fracturing tends to occur in the upper part of the sharp abutment and near the turning point of the abutment slope.
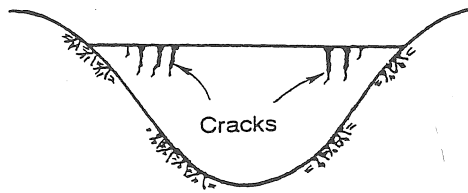
[*] *Professor, Aichi Institute of Technology*
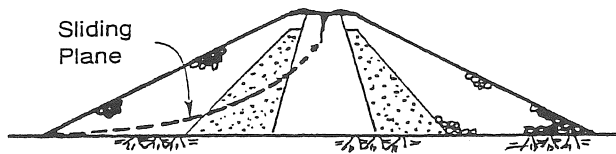[**] *Chief Eng., AICO Consulting co. ltd.*
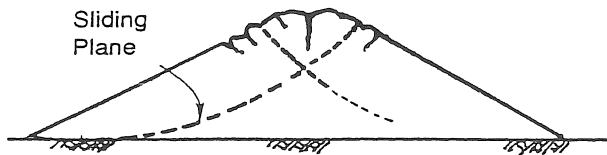[***] *Chief Eng., DAIME Eng. Service co. ltd.*
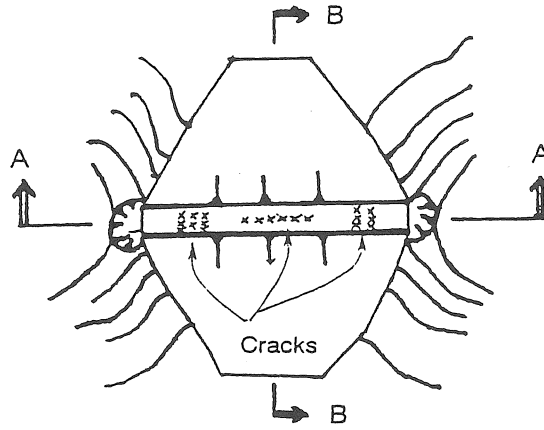
(a) Plan View of Rock Fill Dam

(b) A-A Section

(c) B-B Section

(d) Cracking and Sliding in Earth Dam

Fig.2.1 Damage of Fill-type Dams caused by Earthquake

2. DAMAGE OF FILL-TYPE DAMS CAUSED BY EARTHQUAKE

According to the recent investigation reports on the damages of fill-type dams caused by big earthquakes, seismic damages can be classified into two categories; (1) the transverse cracking at the crest of a dam near the abutment foundation, as shown in Figs.2.1(a) and (b), and (2) the longitudinal cracking to cause sliding failure of embankment slopes, as shown in Figs.2.1(c) and (d).[2] The former type of cracking could lead leakage of the reservoir water and internal erosion through the core.

3. MECHANISM OF HYDRAULIC FRACTURING [3][4]

Hydraulic fracturing takes place due to the decrease in confining stress acting on the soil, which in turn is caused by the differential settlement in the core. In Fig.3.1(a), for instance, differential settlement is induced by the earthquake force near the abutment foundation, and it causes reduction in the lateral confining pressure (σ_3). In Fig.3.2(a), settlement near the turning point of the core width induces arching action and decrease in the vertical confining pressure (σ_1), which must be the cause of hydraulic fracturing. Fig.3.1(b) and Fig.3.2(b), respectively, represents these stress conditions with Mohr's stress circles. As indicated by the dotted lines, reduction in the confining pressure may shift the stress circle left and get it closer to the failure envelope to lead a state of hydraulic fracturing.
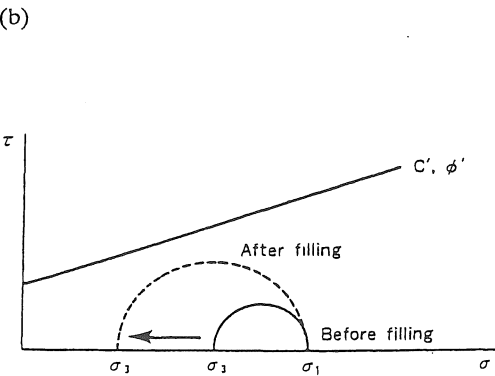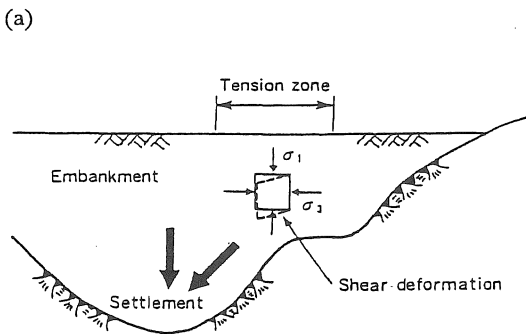
(a)

(b)

Fig.3.1 Stress Change due to Differential Settlement
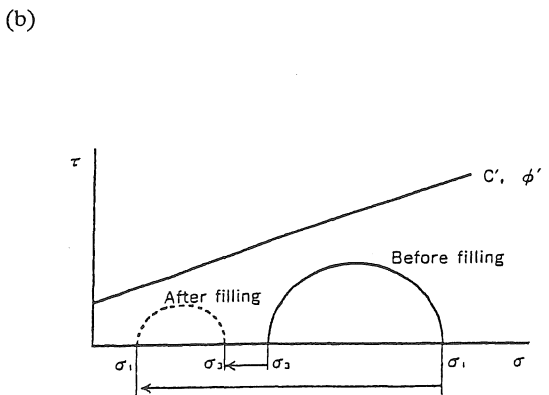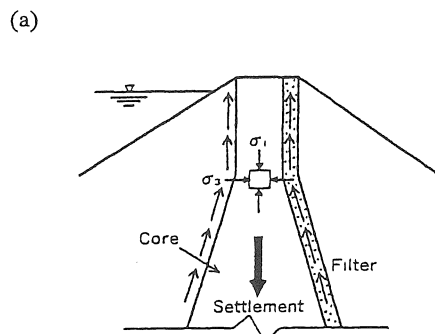
(a)

(b)

Fig.3.2 Stress Change due to Arch Action

3.1 Laboratory tests on hydraulic fracturing

In order to discuss the possibility of hydraulic fracturing for different situations mentioned above, the following two series of tests were carried out in this study.

Test-1: from the initial uniform stress state of $\sigma_1 = \sigma_3$ in the tri-axial compression apparatus, the minor principal stress σ_3 on the specimen is decreased gradually, under a seepage condition of constant hydraulic gradient, to produce the final state of seepage fracture, which realizes the stress states shown in Fig.3.1.

Test-2: seepage fracture tests are conducted under a constant effective vertical stress (σ'_v), by increasing the hydraulic gradient step by step to obtain the final value (i_f) at fracture, which realizes the stress states in presented Fig.3.2.
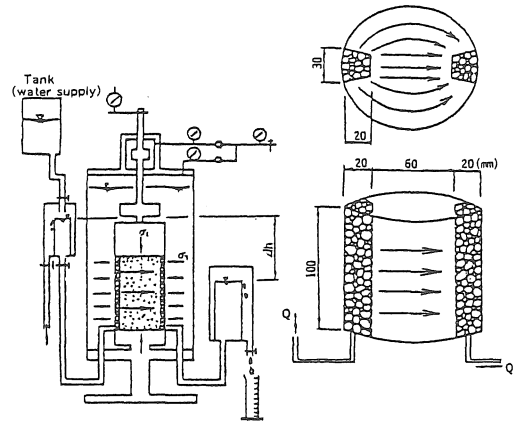
3.2 Apparatus and soil samples

Schematical illustrations of the apparatus for Test-1 and Test-2 series are shown in Fig.3.3 and Fig.3.4, respectively. The water flows from one side to the other in Fig.3.3 and from the center to the two end points in Fig.3.4, with a head difference $\triangle$ h.

Grain size distributions of the materials used in the tests are shown in Fig.3.5, in which the material of a) SM and b) SC are used for Test-1 and Test-2, respectively. The specimens are prepared in the laboratory to satisfy the specified Proctor compaction conditions of dry density and water content, as shown in Fig.3.6, of points B, C and D in Test-1 and the point E in Test-2 series. Details of the test conditions are summarized in Table-3.1.
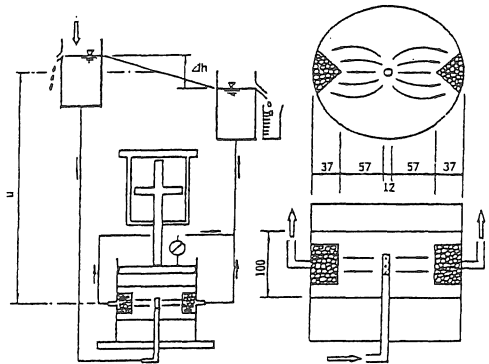
3.3 Test results in Test-1 series

The results of Test-1 series are summarized in Figs.3.7 and 3.8. The relationship between the discharge (q) and the effective stress ratio ($\overline{ob}/\overline{oc}$) defined in the column is shown in Fig.3.8. It is clearly seen in the figure that the discharge from the specimen increases due to the increase in the stress ratio, showing an abrupt

Fig.3.3　Seepage Test Apparatus for Test-1 Series

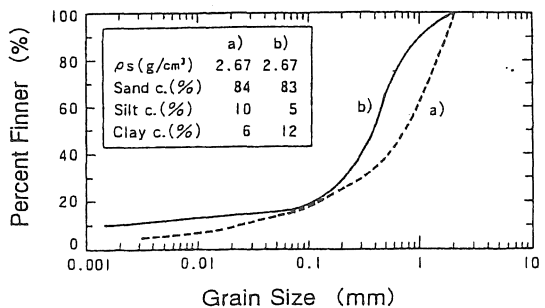Fig.3.4　Seepage Test Apparatus for Test-2 Series

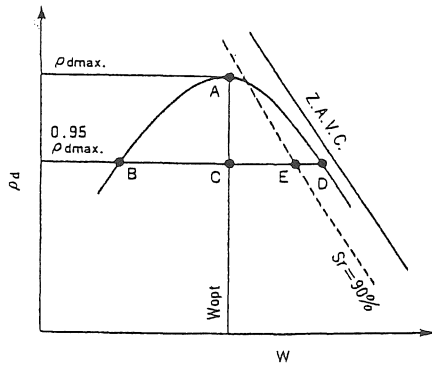Fig.3.5　Grain Size Distribution of Fill Materials used in Tests
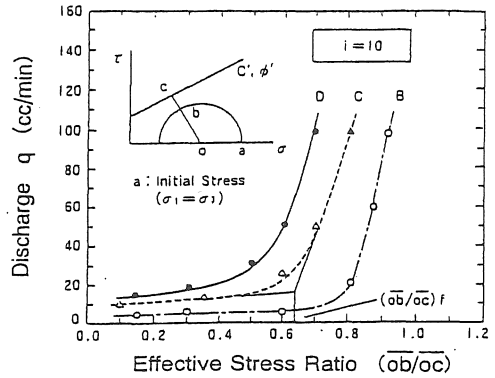
Fig.3.6 Compaction Conditions of Test Specimens

Fig.3.7 Discharge versus Stress Ratio Relation (Test-1)

Table-3.1 Summary of Seepage Test Conditions

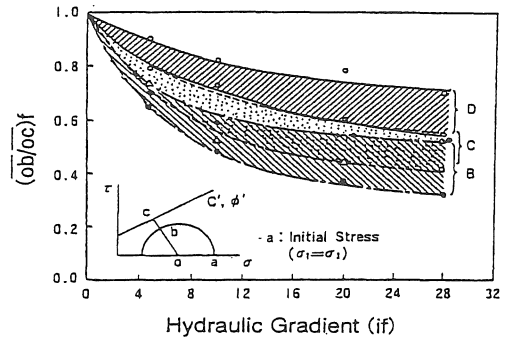|		Test-1	Test-2
Stress and Seepage Conditions		Initial State : $\sigma_1 = \sigma_2$ σ_1 = 1, 2, 3 (kgf/cm') i = 5, 10, 20 σ_3 : gradually decreasing	σ_v = 0.5 (kgf/cm') σ_v'= 0.1, 0.2, 0.4 i : gradually increasing
Specimen	Test Point	B C D	E
	Density	0.95 × ρ_{dmax} (ρ_{dmax} = 1.86g/cm')	0.95 × ρ_{dmax} (ρ_{dmax} = 1.85g/cm')
	Water Content W (%) Deg. of Sat. S_r (%)	9.4 13.7 16.8 49.1 71.6 87.8	17.6 90.0

Fig.3.8 Stress Ratio at Failure (Test-1)

change at a certain condition. The values of the critical stress ratio $(\overline{ob}/\overline{oc})_f$ defined by the point are plotted against the value of the hydraulic gradient at failure (i_f) in Fig.3.8 for different compaction conditions. It is recognized in the figure that for samples having the same dry density a higher resistance can be expected to achieve against hydraulic fracturing as the material is compacted in the wet side of the optimum.

3.4 The test results in Test-2 series

A representative test result of σ'_v = 0.4kgf/cm² is shown in Fig.3.9, taking the discharge (Q) from the specimen on the ordinate and the hydraulic

gradient (i) on the abscissa, in which solid lines are drawn in reference to the constant coefficient of permeability, which satisfies the Darcy's law of v=ki for the state of the laminar flow. It is seen that solid circle plots move along these straight lines of constant k-value in the early stage of the test, showing however an abrupt change in the discharge (Q) in the vicinity of i ≒ 40. The critical value of the hydraulic gradient (i_f) can then be defined at the point of i_f=40 for the case of σ'_v=0.4kgf/cm². The relation between the values of i_f and σ'_v is summarized in Fig.3.10, for the results of the present study by solid circles and for other tests on SM to CL materials by open circles.
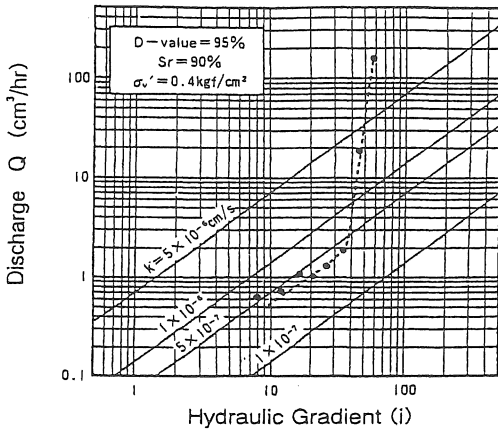
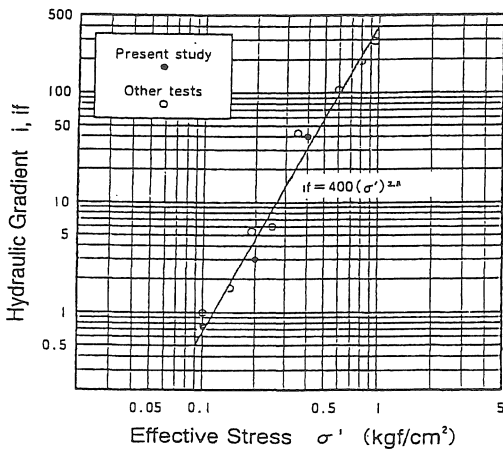Fig.3.9　Discharge versus Hydraulic Gradient Relation (Test-2)

Fig.3.10　Hydraulic Gradient at Failure (Test-2)

4. FEM DYNAMIC RESPONSE ANALYSIS

4.1 Analysis procedure

The aim of this study is to examine the possibility of hydraulic fracturing in fill-type dams when earthquake forces act upon the core with the reservoir filled with water. FEM dynamic response analysis is now conducted on simple embankment models for different types of harmonic excitation. Analysis procedures and conditions employed here are summarized below.

1) The analysis is done for a standard type of rock fill dam with a centrally located core of 100m in height, as presented in Fig.4.1, by changing abutment configuration in four cases.

2) Two-dimensional analysis may be reasonable as a first step to understand dynamic behavior of fill-type dams and to evaluate their possibility of hydraulic fracturing during earthquake. Analysis is therefore made for harmonic excitation of acceleration with a frequency of 1Hz.

3) The analytical procedure adopted here is basically the same as the QUAD-4 program, where non linear material properties of dynamic behavior are represented by the Hardin-Drnevich model in the following forms.

$$G/G_0 = \frac{1}{1 + (\gamma / \gamma_r) \gamma}$$

$$h/h_0 = \frac{\gamma / \gamma_r}{1 + (\gamma / \gamma_r)}$$

where $\quad G_0 = 510 \; \sigma'^{0.47}$

$\quad\quad\quad \gamma_r = 4.8 \times 10^{-3} \; \sigma'^{0.75}$

4.2 Results of dynamic response analysis

1) Dynamic response of embankment

In Table-4.1, values of the input and response acceleration calculated at the base and the crest are compared, with the natural frequency obtained for the primary mode of vibration of the embankment. It is clear that the response acceleration at the crest is about 3.5 to 4.0 times larger than the base acceleration.

Primary mode of vibration and distribution of the response acceleration in embankment are drawn in Fig.4.2 for a representative case of the abutment slope of 1 to 1.5 (case-2). Such results for others cases as case-1, 3, 4 and 5 are almost same as that of case-2 one's.

2) Evaluation of hydraulic fracturing

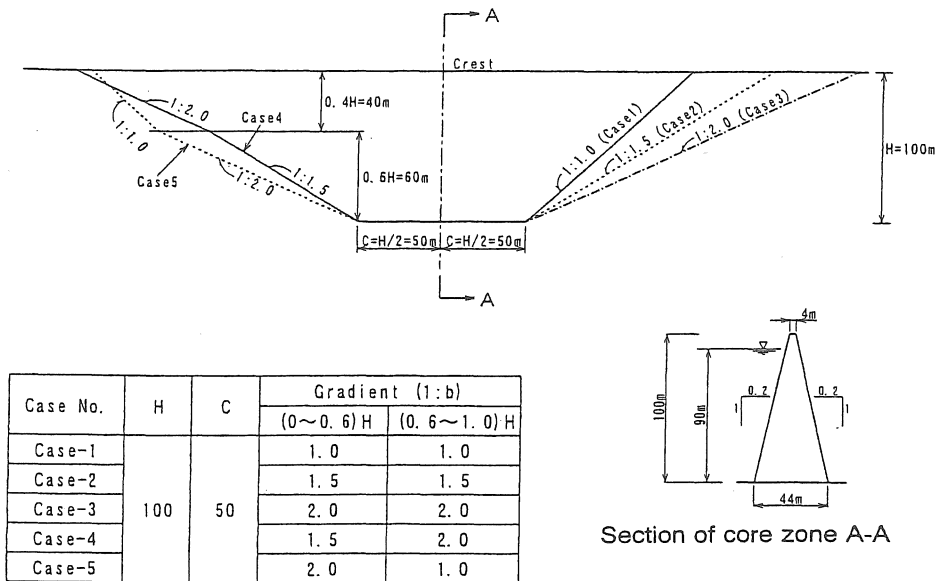Possibility of the hydraulic fracturing during earthquake is examined here by applying the following two criteria.

Fig.4.1 Abutment Configuration Employed in Dynamic Response Analysis

Case No.	H	C	Gradient (1:b)	
			(0~0.6)H	(0.6~1.0)H
Case-1			1.0	1.0
Case-2			1.5	1.5
Case-3	100	50	2.0	2.0
Case-4			1.5	2.0
Case-5			2.0	1.0

Section of core zone A-A

Table 4.1 Response Acceleration at Dam Crest

Case No.	Base Acceleration （1Hz）		
	50 gal	100 gal	200 gal
Case-1	214.3 (1.05)	414.5 (1.02)	754.9 (0.97)
Case-2	218.4 (0.95)	407.8 (0.93)	707.6 (0.90)
Case-3	200.9 (0.90)	373.1 (0.89)	667.7 (0.86)
Case-4	200.9 (0.90)	372.6 (0.89)	666.1 (0.86)
Case-5	201.9 (0.91)	373.6 (0.89)	666.7 (0.86)

( ) shows natural frequency (Hz) at the first mode

N-1550-U2

N-1550-U4

N-1550-U6

N-1550-U8

N-1550-U10

N-1550-U12

N-1550-U14

N-1550-U16

$\alpha_b = 50\,\mathrm{gal}$

1sec

Disp. Scale
0   5   10cm

Model Scale
0   50   100m

Accel. Scale
0   500gal

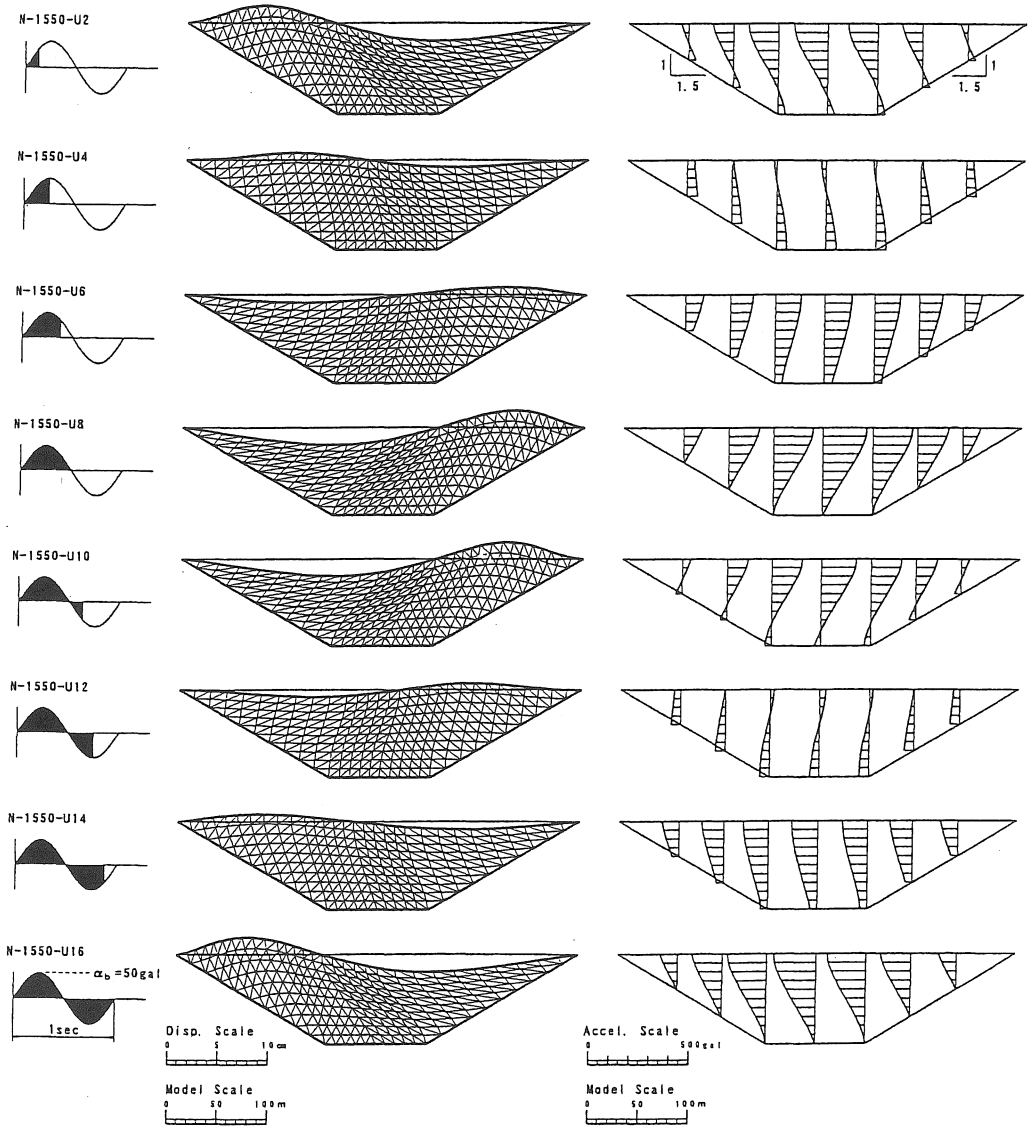Model Scale
0   50   100m

Fig.4.2   Deformation mode along dam axis

(a) Safety evaluation proposed in this paper

Evaluation of safety factor against hydraulic fracturing is explained in Fig.4.3, which is redrawn from Fig.3.8 in a more precise form. In this figure, the stress ratio which leads to hydraulic fracture is obtained corresponding to the value of the hydraulic gradient at failure (i_f), and the safety factor can be evaluated as the ratio of the value of the stress ratio at failure to that at the present state. Assuming that $i_f = 2.0$ for the soil compacted in the state of B, for example, the value of the stress ratio at failure can be determined from the upper solid line as $(\overline{\sigma b/\sigma c})_f = 0.95$. If the value of the stress ratio calculated in the dynamic response analysis is taken as $(\overline{\sigma b/\sigma c}) = 0.93$, the safety factor (F_s) becomes to be $F_s = 0.95/0.93 \fallingdotseq 1.02$, suggesting a little safety against hydraulic fracturing.

(b) Safety evaluation by Seed[5),6)]

Seed et al. (1976) have presented the following criteria to evaluate possibility of hydraulic fracturing in the Teton dam failure.

$$\sigma_3' \leqq u$$

where σ_3' and u are the minor principal stress and pore water pressure, respectively, at a certain point.
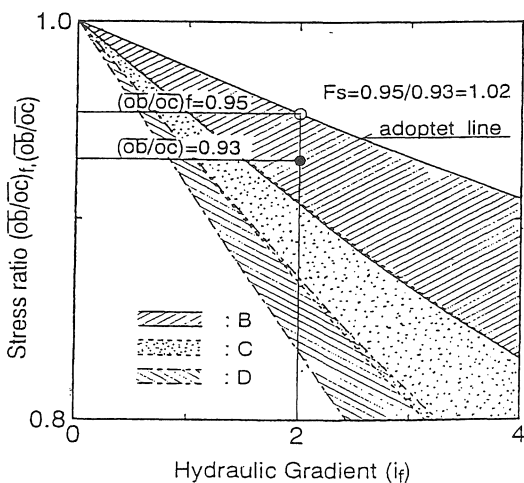

Fig.4.3 Safety Evaluation with Stress Ratio

5. DISCUSSIONS ON POSSIBILITY OF HYDRAULIC FRACTURING

Possibility of hydraulic fracturing in the core zone is discussed now by comparing the results from two methods of safety evaluation presented above; one is the criterion proposed in this paper and the other by Seed et al.

5.1 Safety evaluation proposed in this paper

Distributions of the response acceleration and the safety factor against hydraulic fracturing in the embankment are presented in Fig.5.1 through Fig.5.10 for all cases of abutment configuration. Discussions are summarized in the following.

(a) In the embankment with abutment slope of 1:1.5, hydraulic fracture appears initially in the upper part near the abutment foundation, and it develops to the lower part as the response acceleration increases.

(b) Possibility of fracturing becomes lower as the abutment slope is gentle.

(c) In the case the abutment foundation has a turning point of slope inclination, hydraulic fracture takes place first near the point and it extends widely upwards.

(d) In the case the abutment slope is steeper in the upper part than the lower (U-shaped valley), fracture starts near the turning point of slope and it extends upwards and much more widely than the above case along the upper steep abutment. This result is not a matter of worrying about, because the confining stress in the core is much higher than the above case in the static state.

5.2 Safety evaluation by Seed method

Distributions of the minor principal stress σ_3 and the pore water pressure u in embankment are given in Fig.5.11 through Fig.5.15. Tendency of hydraulic fracturing is almost the same as presented above except the shape and extent of the rapture zone. It is clear that the criterion presented by Seed is rather loose as compared with that proposed in this paper.

6. SUMMARIES

Possibility of hydraulic fracturing during earthquake was discussed in this paper through laboratory seepage fracture tests and FEM dynamic response analysis. Focus of the present study is placed on to know the threshold of the hydraulic fracturing, and satisfactory results were obtained to discuss on the safety evaluation of embankment against hydraulic fracture. It is necessary, however, much more follow-up study to apply the proposed method for the actual dam design: i.e., more rigorous 3D dynamic analysis and seepage fracture tests under vibration are required for a future precise study on hydraulic fracture.

REFERENCES

1) Ohne, Y. et al (Nov. 1996). Evaluation of seismic slope stability of earth and rock fill dams, *First U.S-Japan Workshop on Advanced Research on Earthquake Eng. for Dams*.

2) Ohne,Y. （1985）. Seismic behavior of MAKIO dam, *A report of specialty session of NAGANO-KEN SEIBU Earthquake, the 20th JSSMFE annual meeting*. （in Japanese）

3) Ohne, Y. & Narita, K. (1978). Some considerations of the Teton Dam failure. *Technical report of Aichi Inst. of Technology,* No.13: pp.217-229.

4) Murase, Y. et al (Aug. 1995). Study on hydraulic fracturing of core-type rock fill dams. *The MWA International Conf. on Dam Engineering*, pp.363-371.

5) Teton Dam Failure Interior Review Group. 1976a. *First interim report on the Teton Dam failure.*

6) Teton Dam Failure Interior Review Group. 1976b. *Second interim report on the Teton Dam failure.*

7) Narita, K. et al （1997）. Centrifuge model tests on hydraulic fracturing in earth and rockfill dams. *Proc. 9th Int. Conf. of IACMAG*, vol.3, pp.2291-2294.
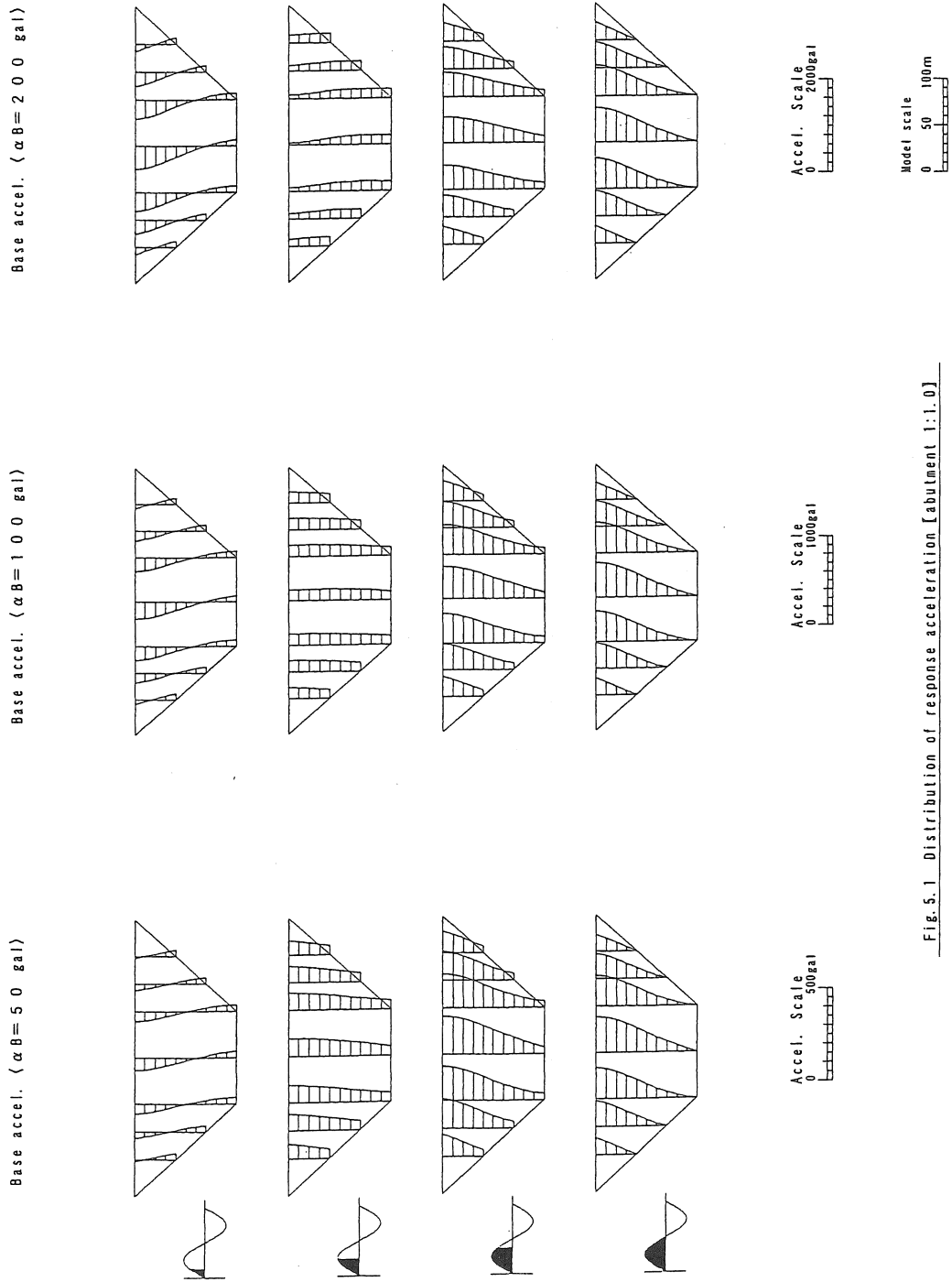
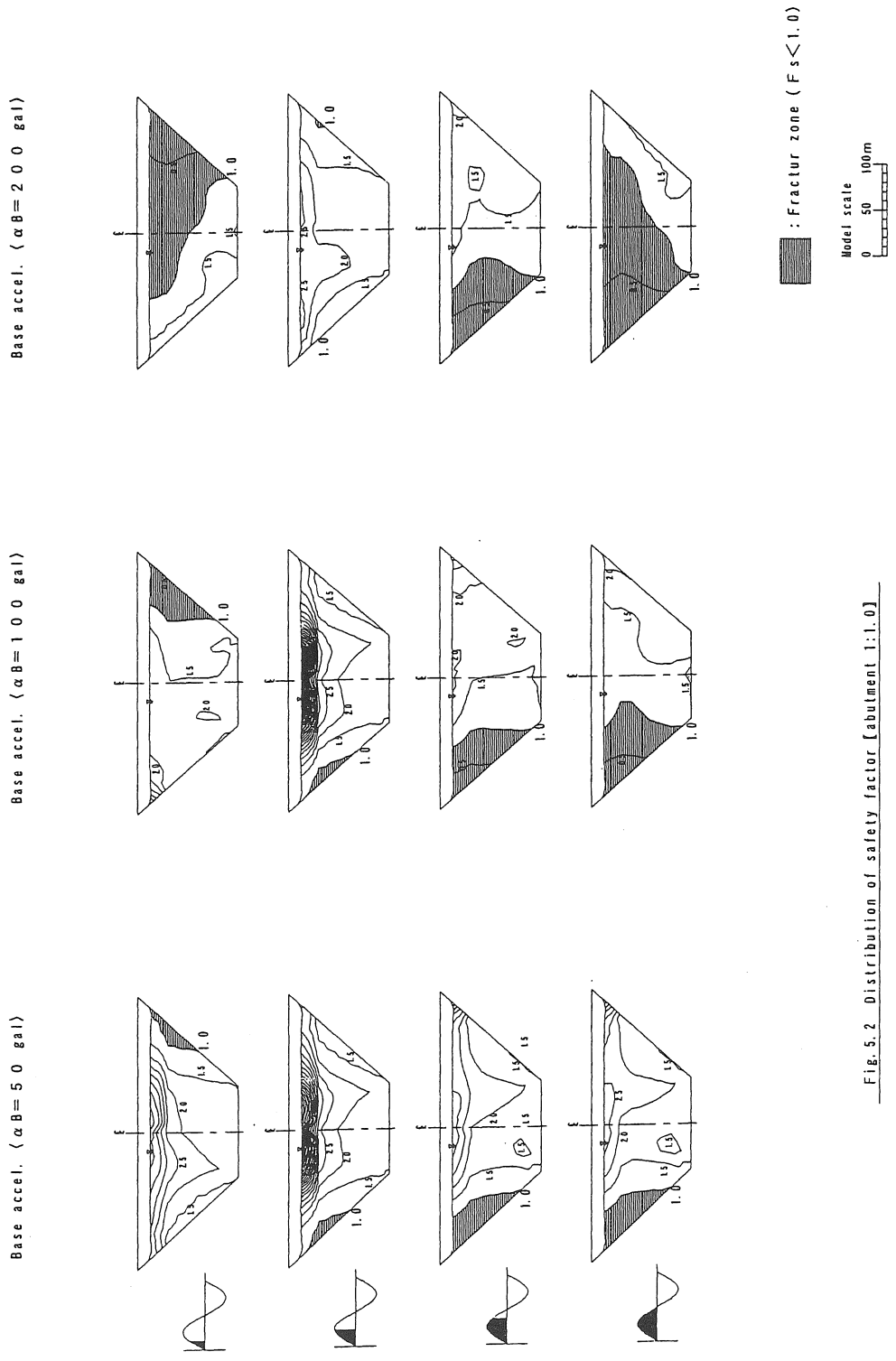Fig. 5. 1 Distribution of response acceleration [abutment 1:1. 0]

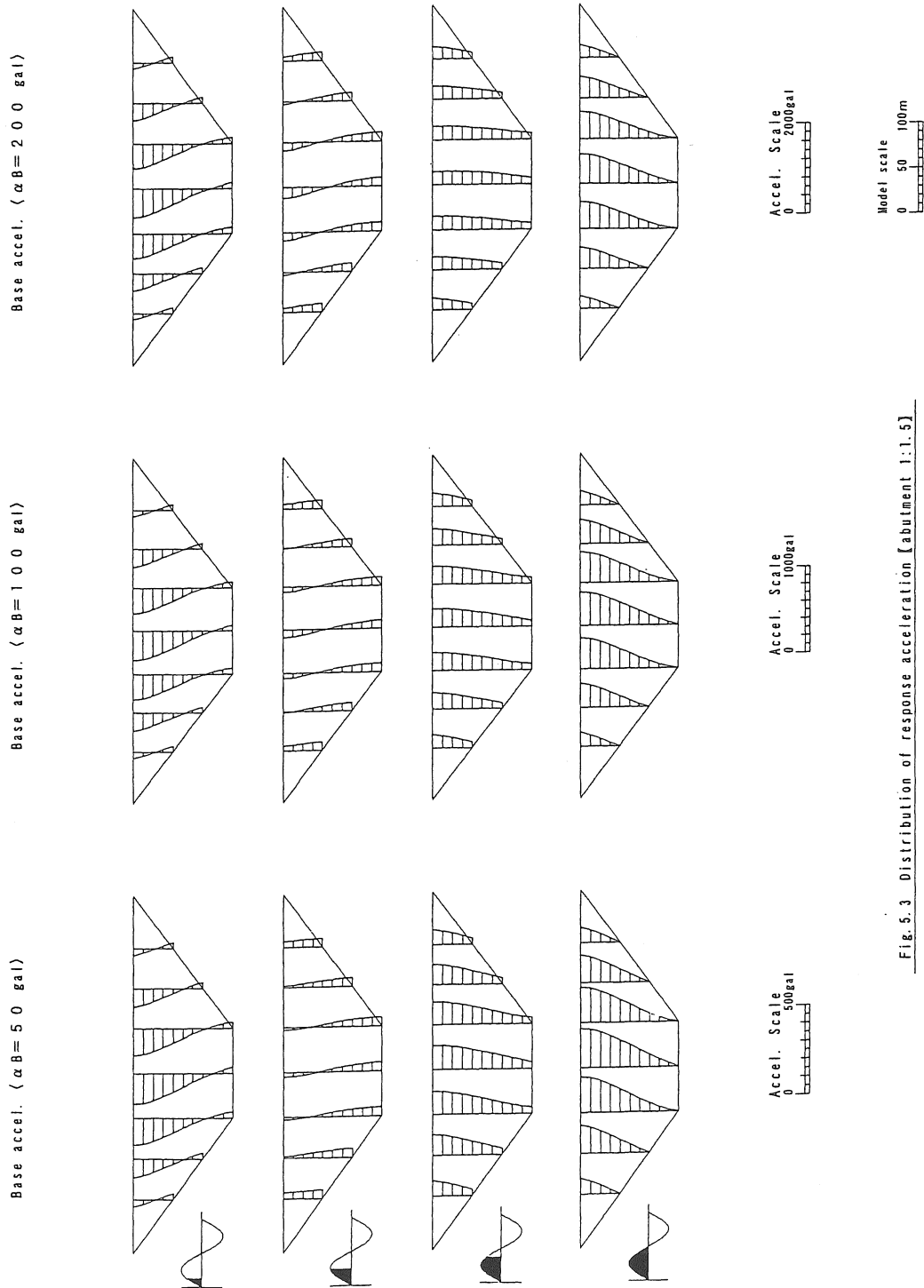Fig. 5.2 Distribution of safety factor [abutment 1:1.0]

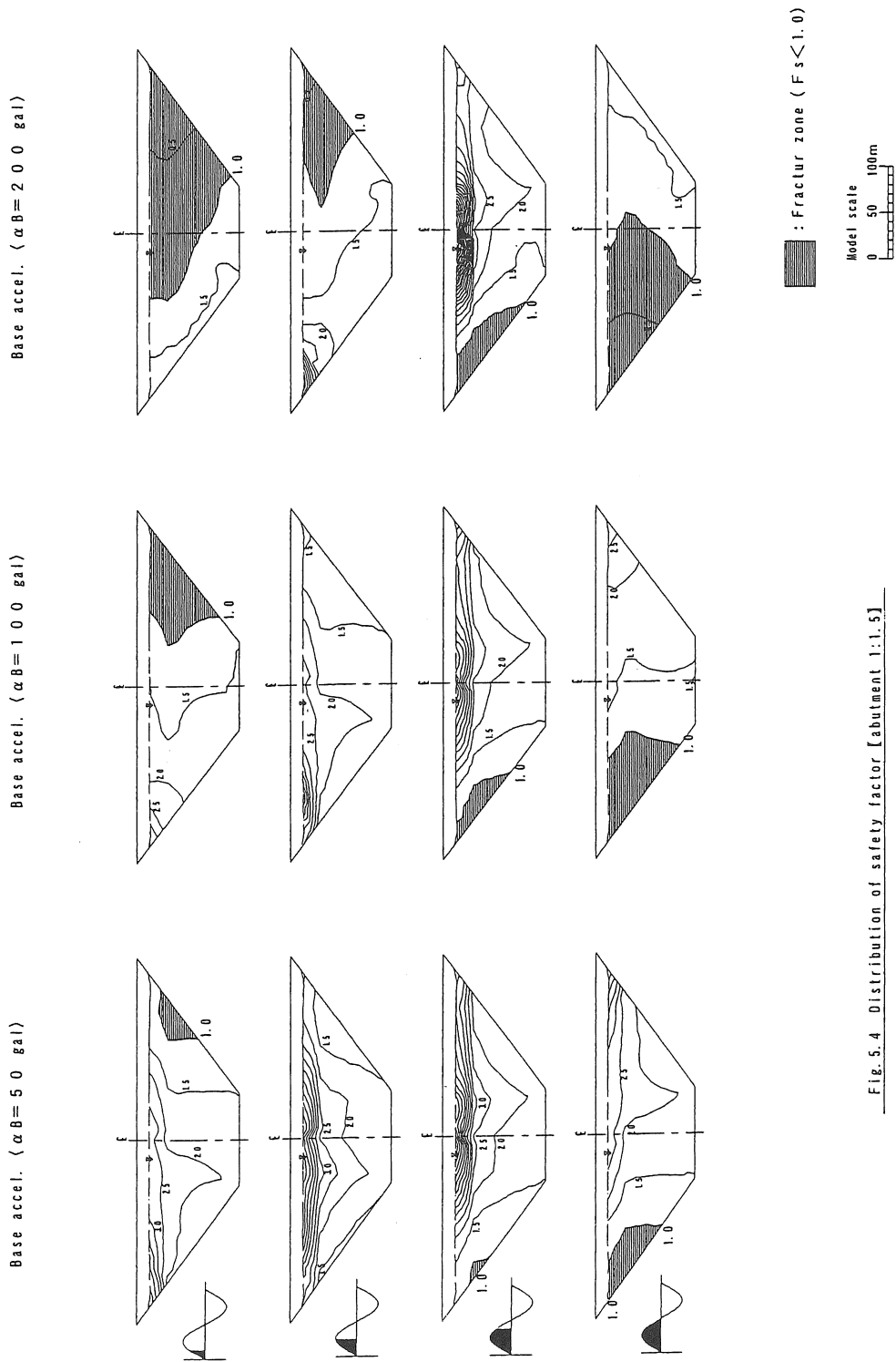Fig. 5.3 Distribution of response acceleration [abutment 1:1.5]

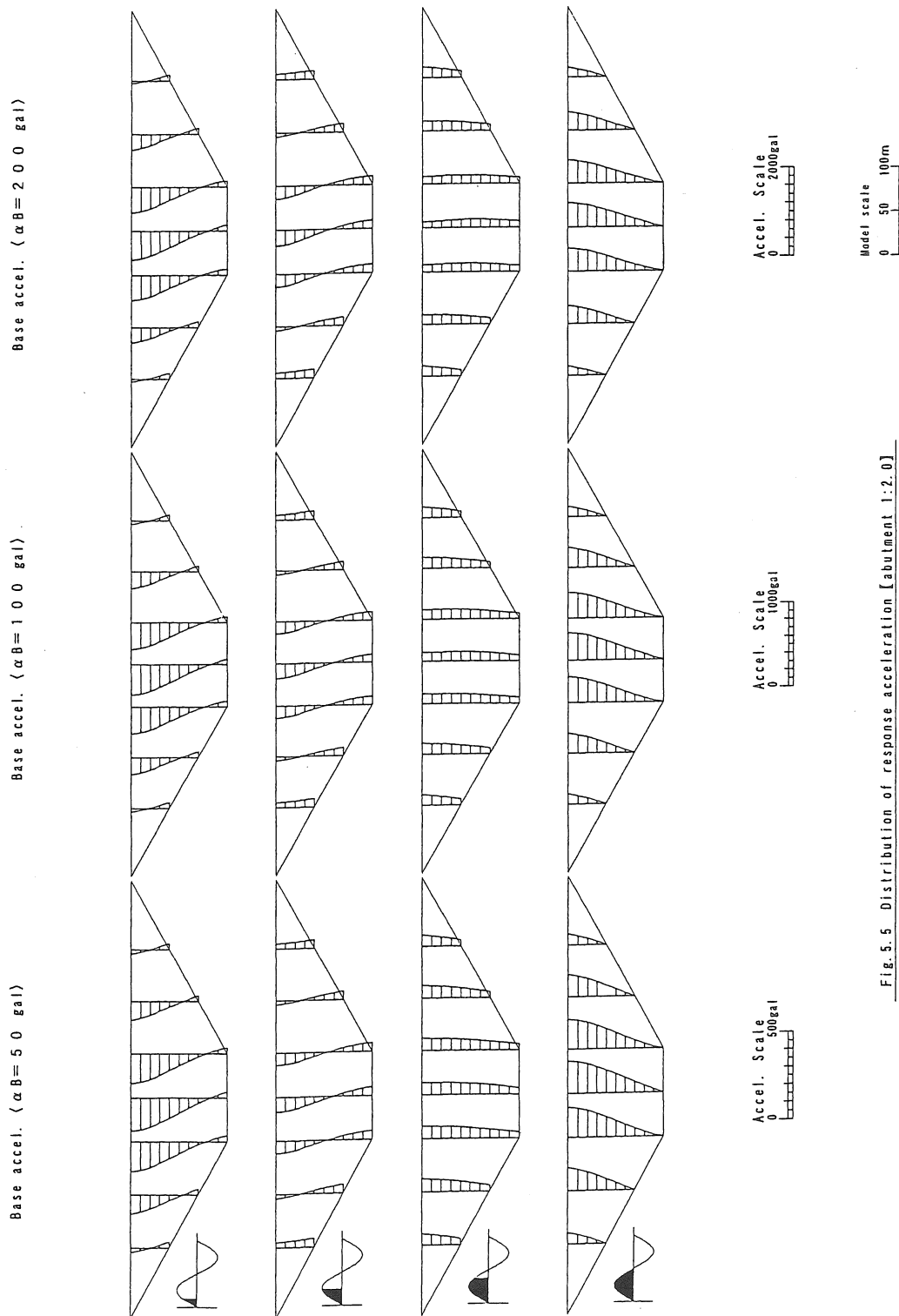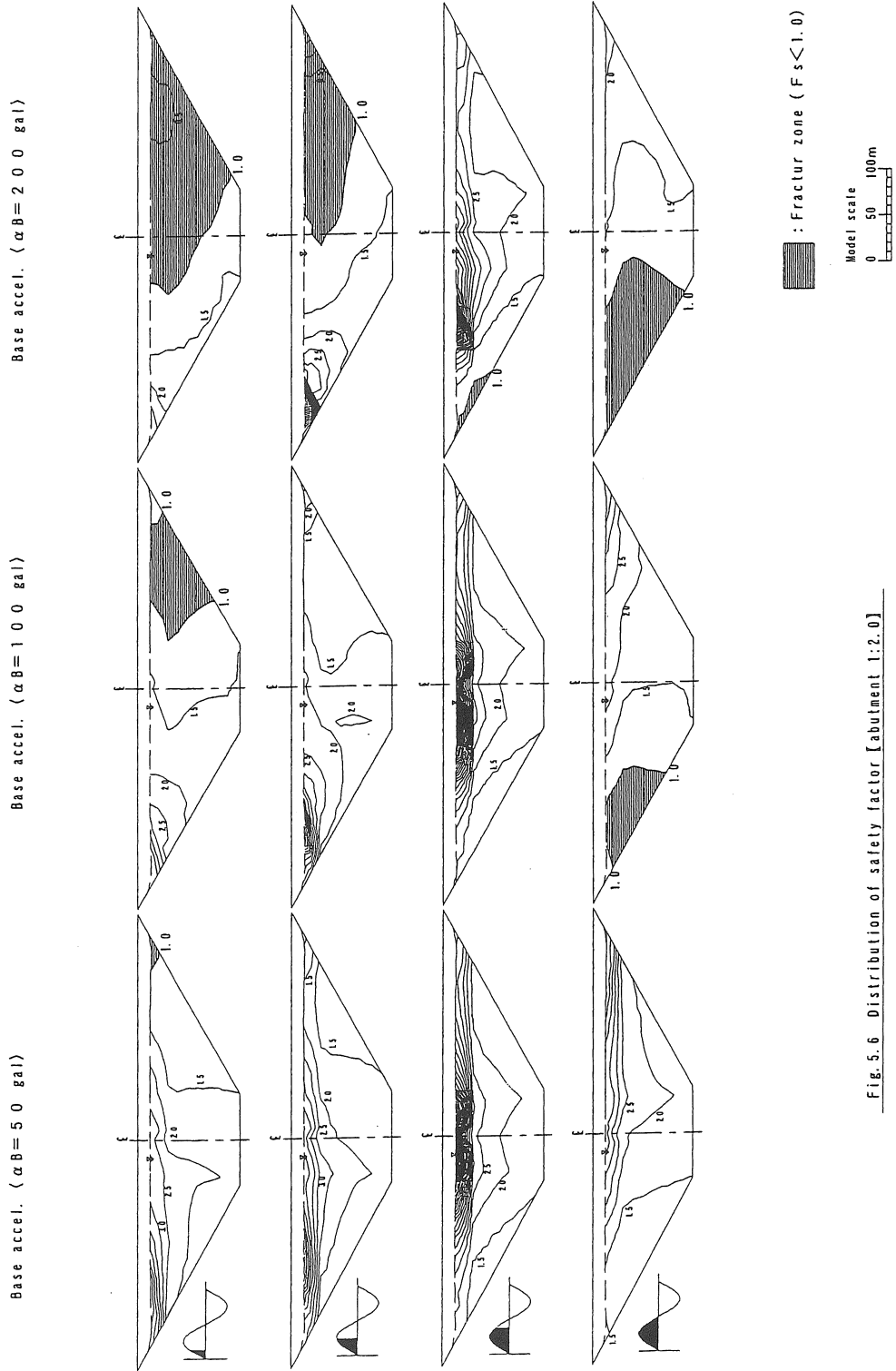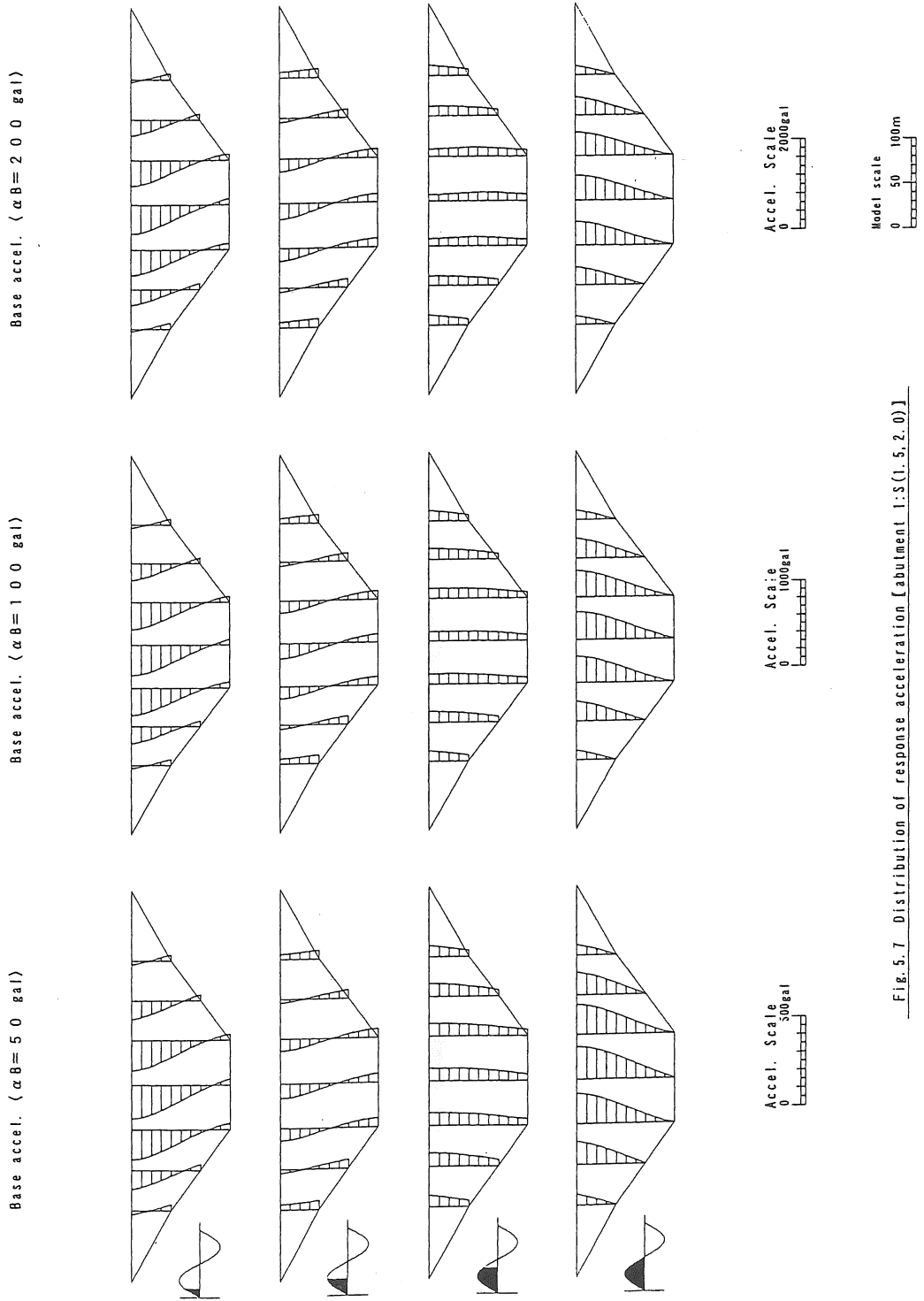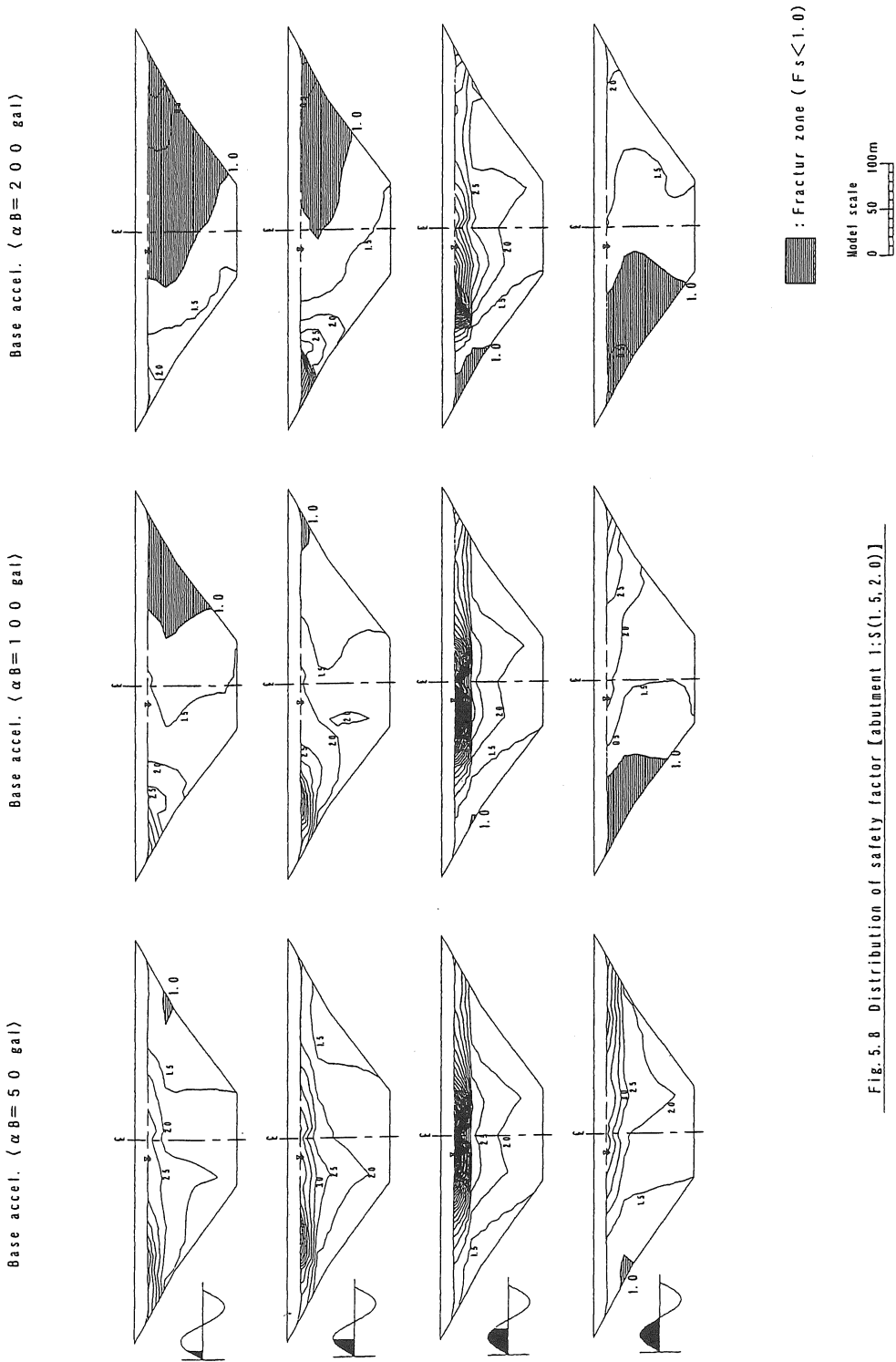Fig. 5.4 Distribution of safety factor [abutment 1:1.5]

Base accel. 〈αB= 5 0 gal〉

Base accel. 〈αB= 1 0 0 gal〉

Base accel. 〈αB= 2 0 0 gal〉

Accel. Scale
0   500gal

Accel. Scale
0   1000gal

Accel. Scale
0   2000gal

Model scale
0   50   100m

Fig. 5. 5   Distribution of response acceleration [abutment 1:2. 0]

Fig. 5.6　Distribution of safety factor [abutment 1:2.0]

Fig. 5.7 Distribution of response acceleration [abutment 1:S(1.5,2.0)]

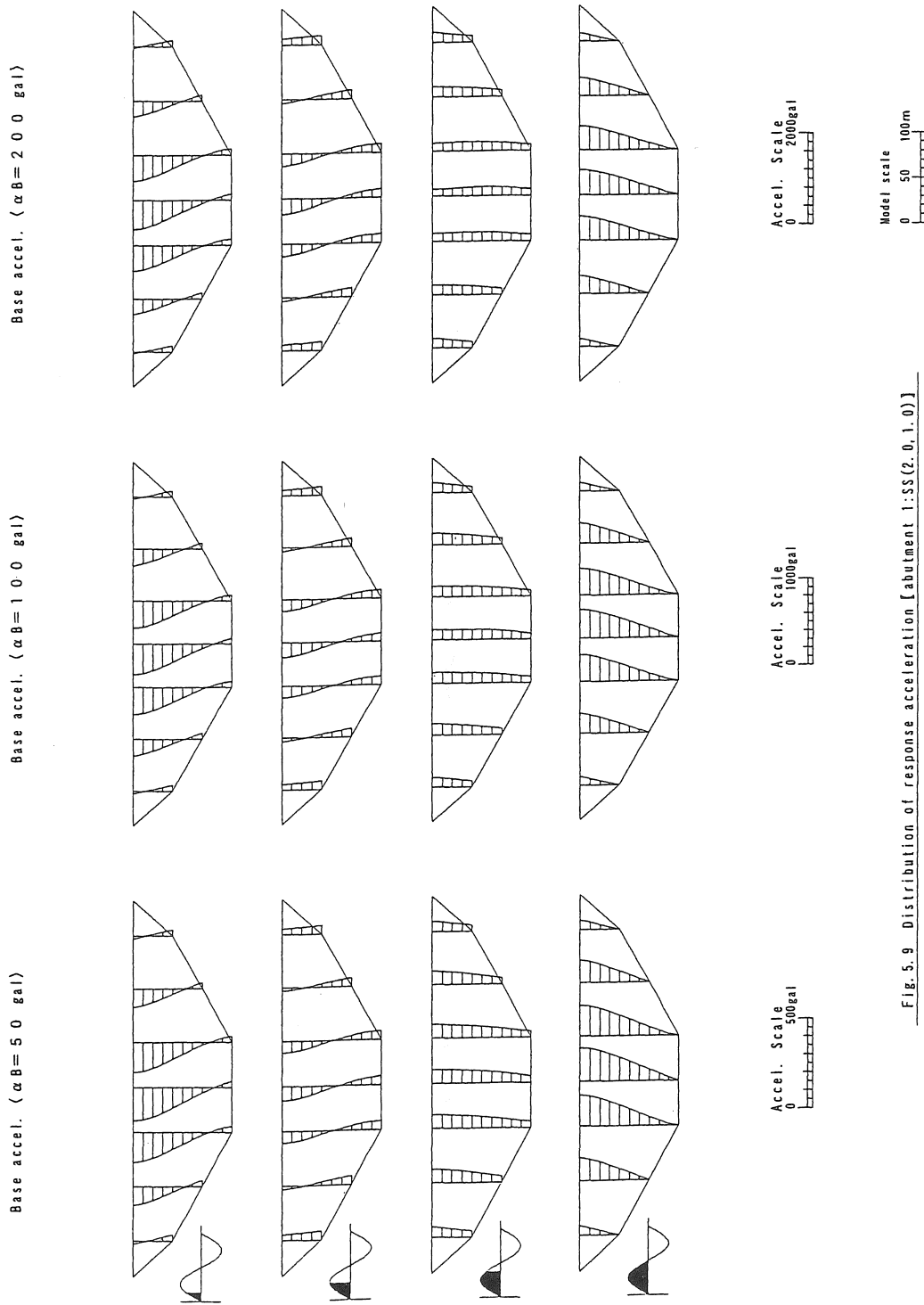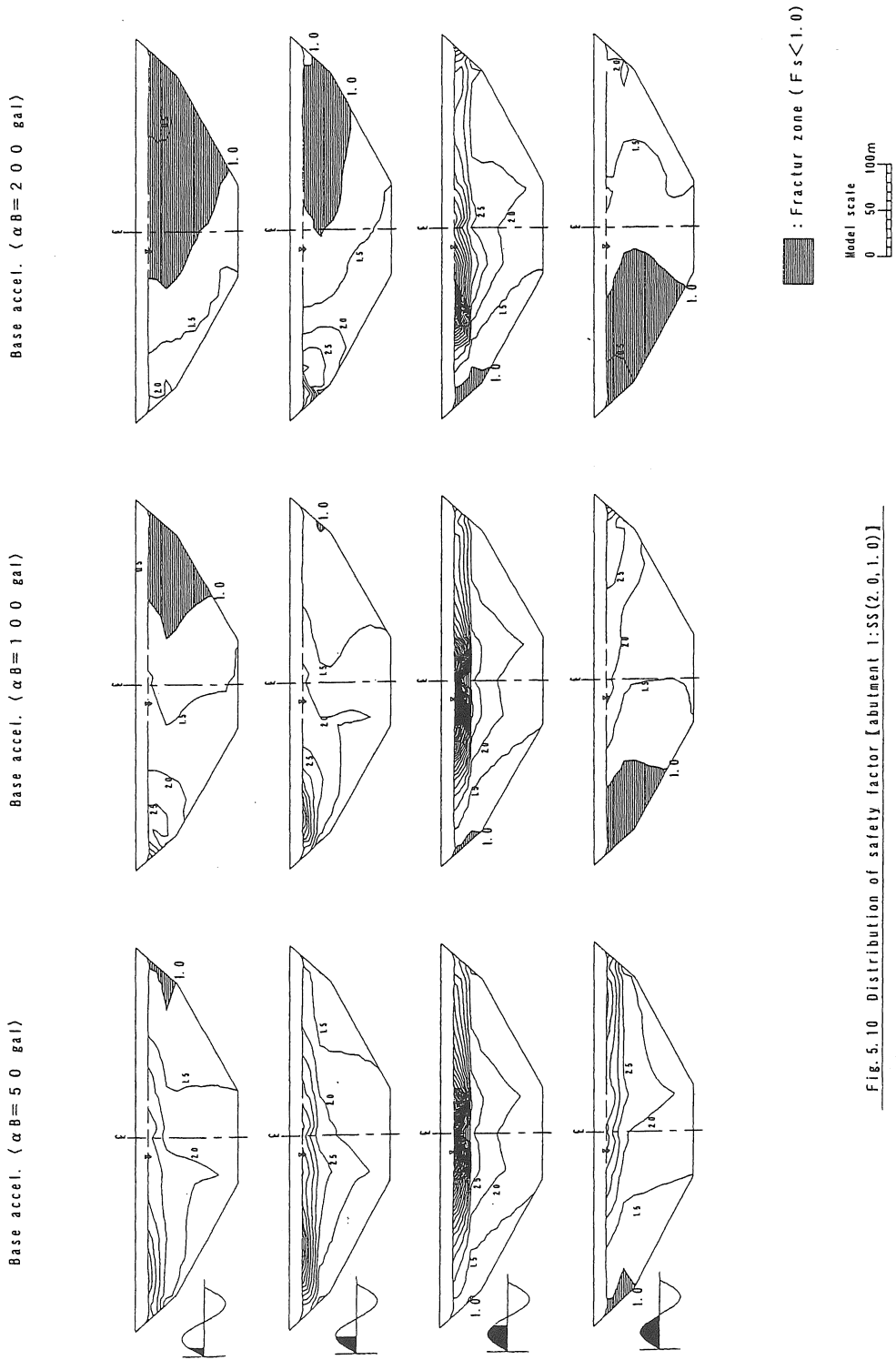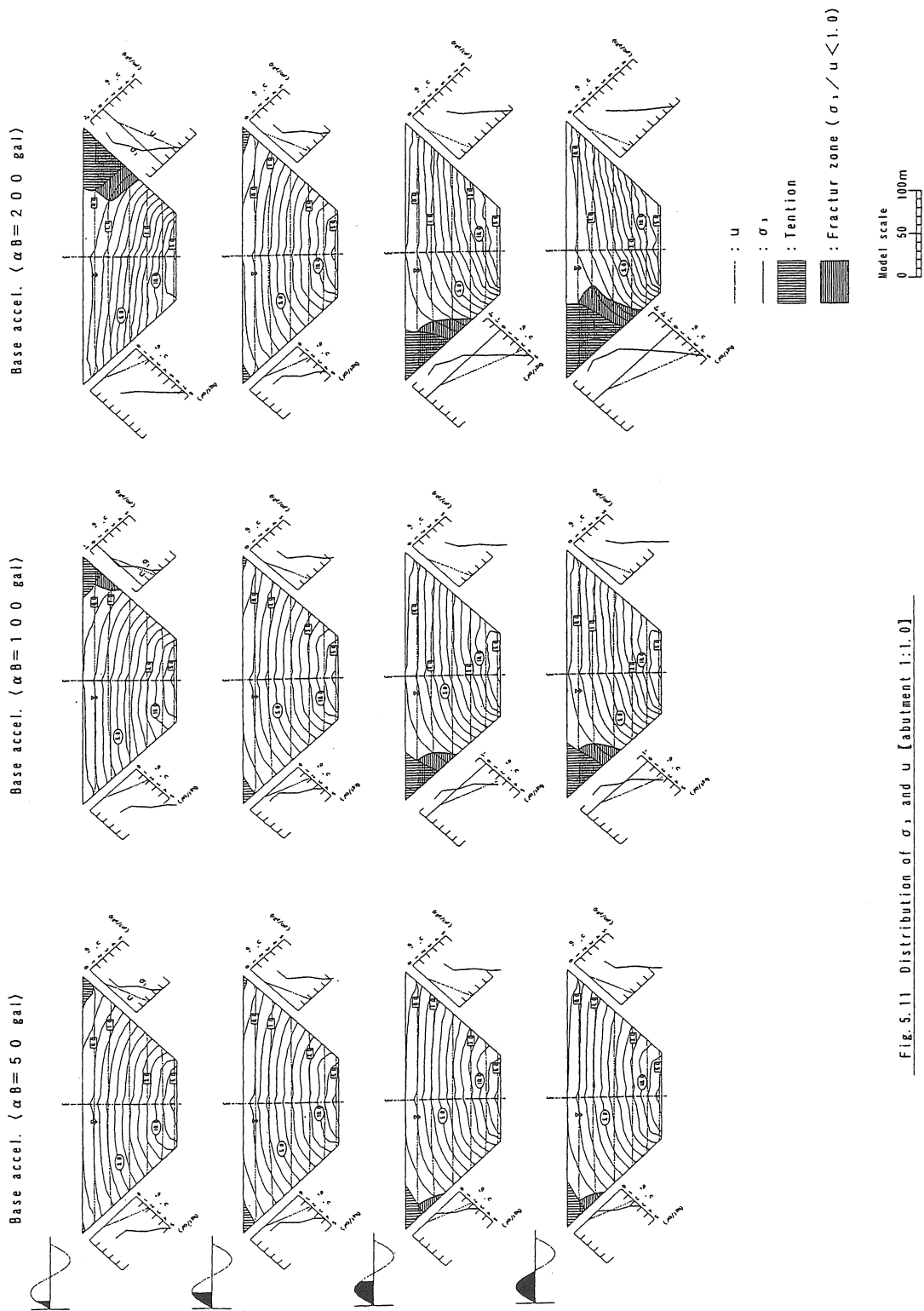Fig. 5. 8　Distribution of safety factor [abutment 1:S(1. 5, 2. 0)]

Base accel. (αB＝200 gal)

Base accel. (αB＝100 gal)

Base accel. (αB＝50 gal)

Accel. Scale
0　2000gal

Accel. Scale
0　1000gal

Accel. Scale
0　500gal

Model scale
0　50　100m

Fig. 5.9　Distribution of response acceleration [abutment 1:SS(2.0,1.0)]

Base accel. 〈αB＝200 gal〉

Base accel. 〈αB＝100 gal〉

Base accel. 〈αB＝50 gal〉

: Fractur zone (Fs＜1.0)

Model scale

0　　50　　100m

Fig. 5.10　Distribution of safety factor [abutment 1:SS(2.0, 1.0)]

Fig. 5.11 Distribution of σ_1 and u [abutment 1:1.0]

Base accel. 〈αB＝200 gal〉
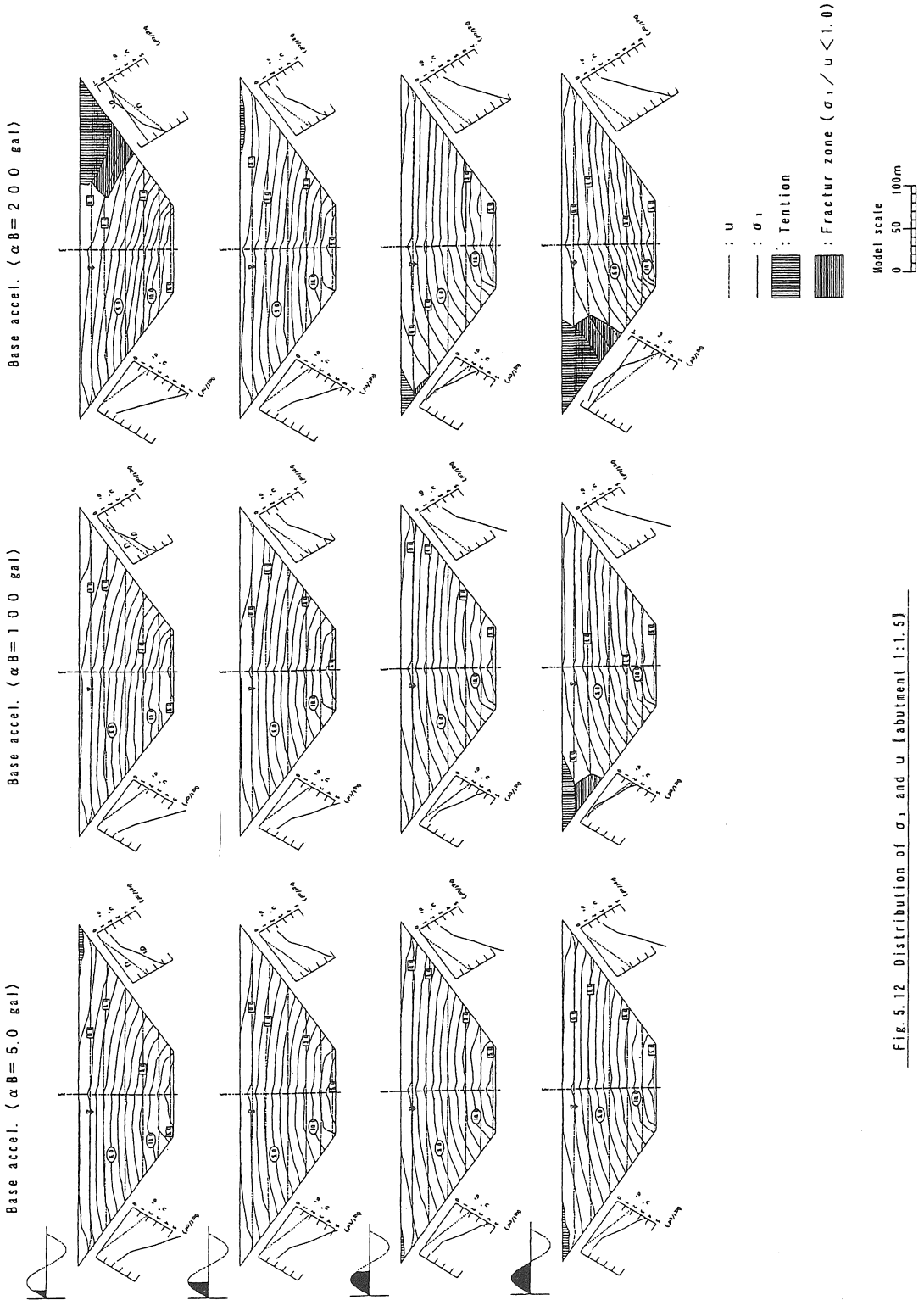
Base accel. 〈αB＝100 gal〉

Base accel. 〈αB＝5.0 gal〉

: u

: σ₁

: Tention

: Fractur zone (σ₁／u ＜1.0)

Model scale

0　　50　　100m

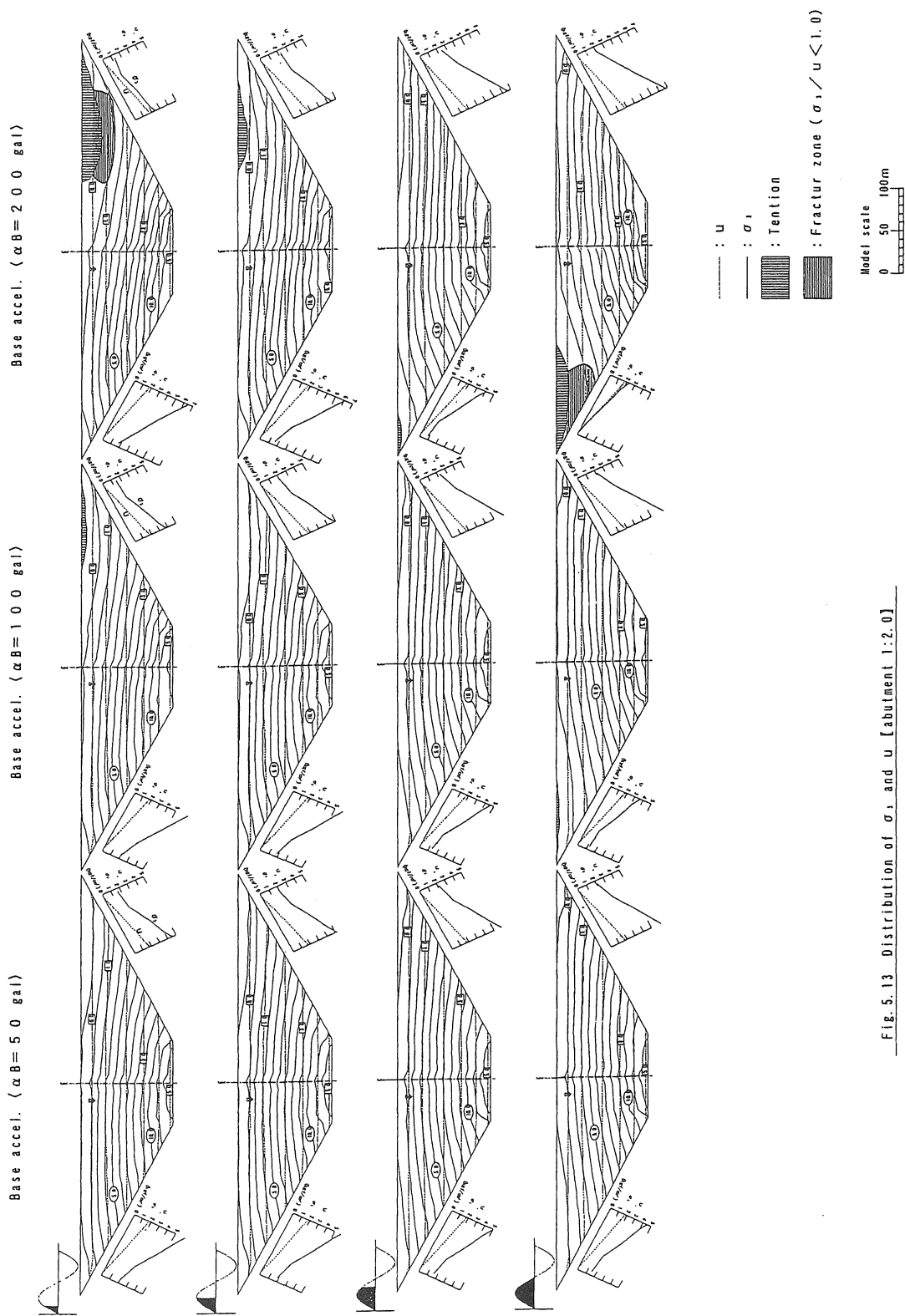Fig. 5.12　Distribution of σ₁ and u [abutment 1:1.5]

Fig. 5.13 Distribution of σ_1 and u [abutment 1:2.0]
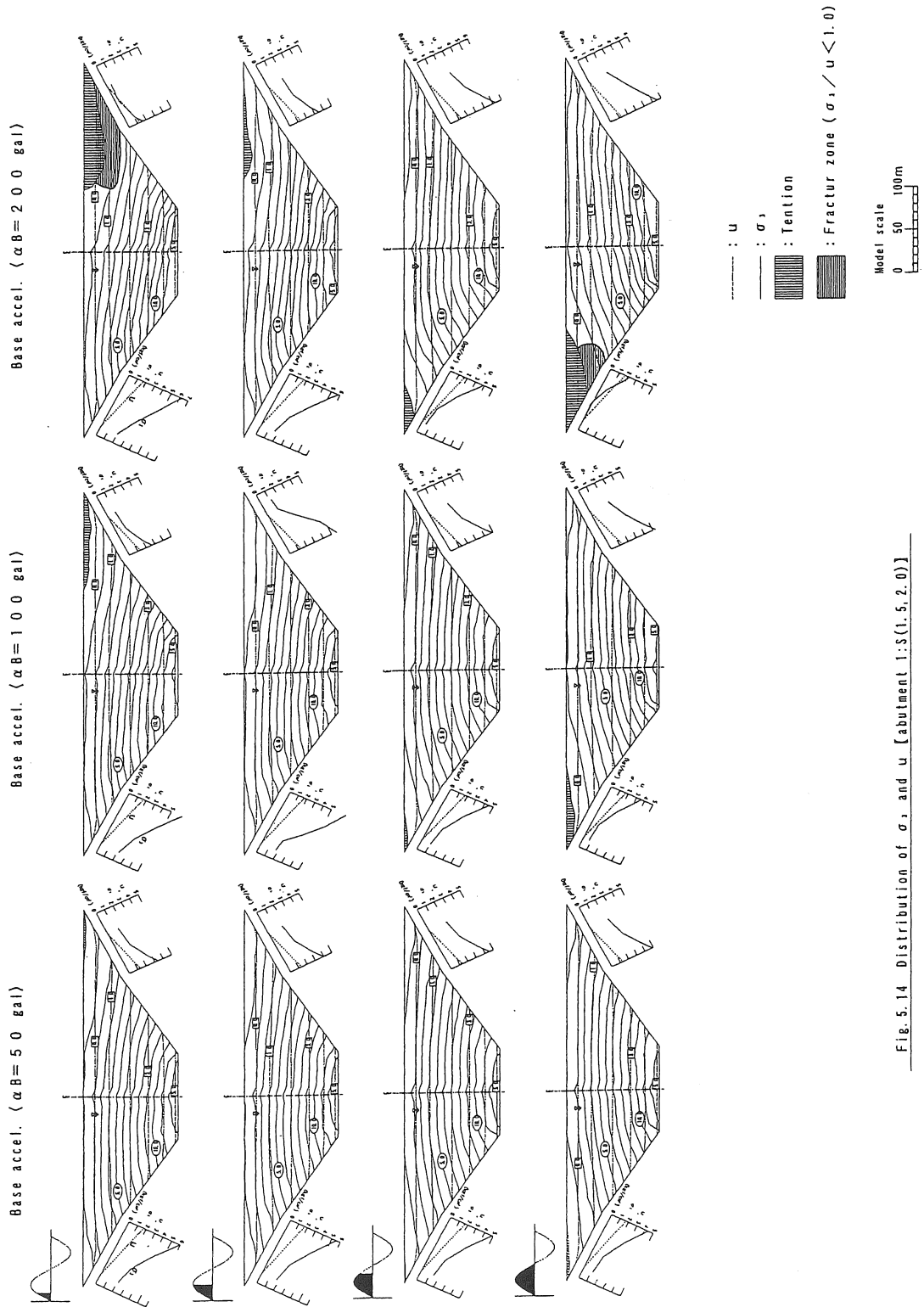
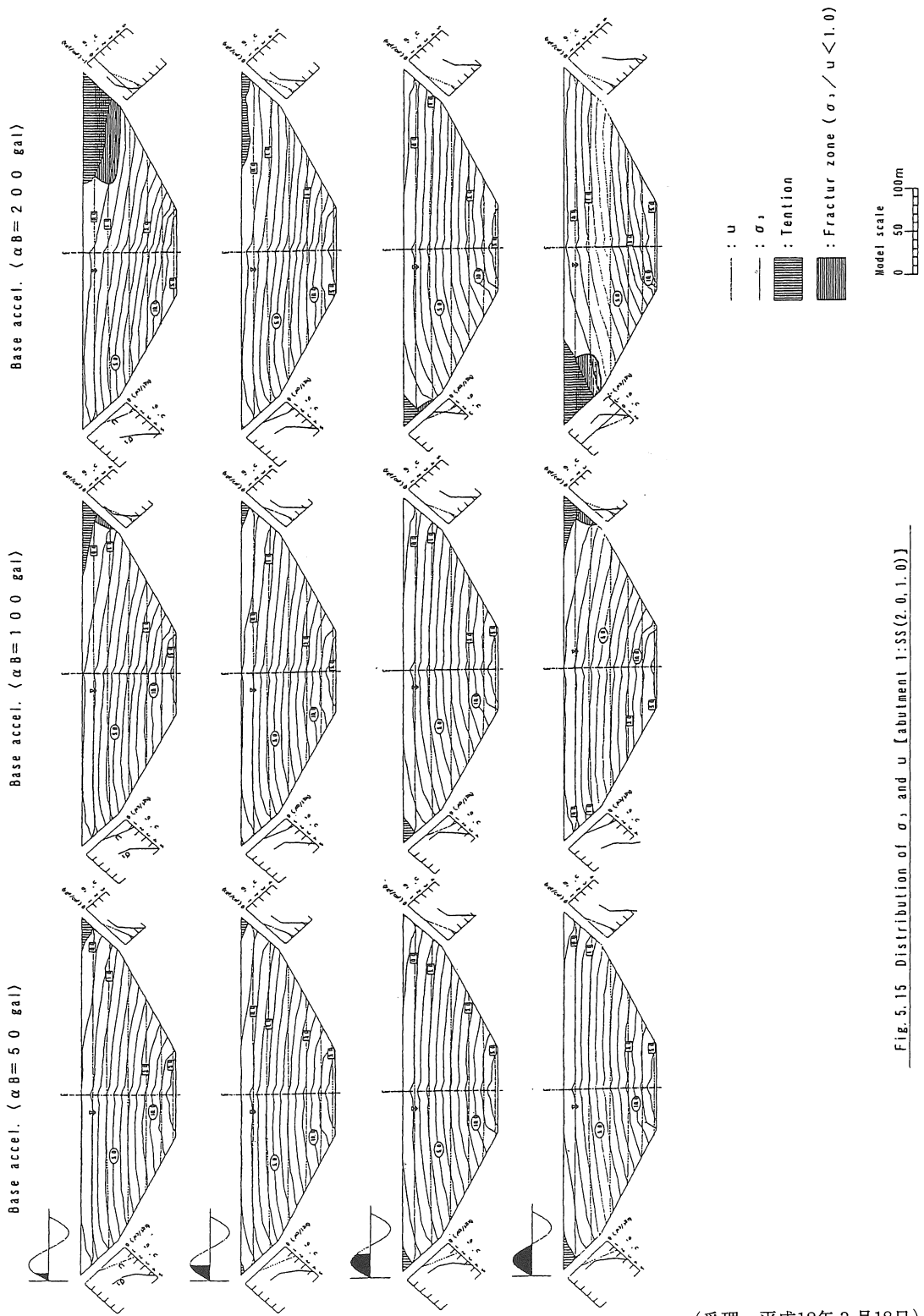Fig. 5.14　Distribution of σ_3 and u [abutment 1:S(1.5, 2.0)]

Fig. 5.15 Distribution of σ_3 and u [abutment 1:SS(2.0.1.0)]